Synthesis and characterization of novel triazeno-group containing photopolymers

Oskar Nuyken, Jürgen Stebani*[a]

Lehrstuhl für Makromolekulare Stoffe, Technische Universität München, D-85747 Garching, Germany

Thomas Lippert[b], *Alexander Wokaun*

Lehrstuhl für Physikalische Chemie II, Universität Bayreuth, D-95440 Bayreuth, Germany

Andrej Stasko

Physical Chemistry, Slovak Technical University, 81237 Bratislava, Slovakia

(Received: March 21, 1994; revised manuscript of June 17, 1994)

SUMMARY:

The synthesis of novel triazeno-group containing photopolymers is described including their characterization by spectroscopic methods, differential scanning calorimetry, and thermogravimetric analysis. Triazene polymers synthesized by a polycondensation reaction between a bis-diazonium salt and a bifunctional secondary amine are well soluble in usual organic solvents. Transparent, light yellow films of these photopolymers may be produced by simple spin-coating and solution-casting techniques. The effect of polymer structural elements on the photolytic decomposition is studied. Depending on the structure of the polymer, thermolysis proceeds either via a one-step or two-step mechanism.

Introduction

Considerable attention has been directed over the last two decades to the effect of ultraviolet (UV) radiation on polymer systems. UV radiation is known to affect most polymer materials by the creation of excited states and free radicals, which are capable of initiating a large number of reactions such as chain scission, (zip) depolymerization, crosslinking, oxidation, or secondary polymerization reactions[1]. After powerful UV laser systems had become available in the early 1980's, investigations focused on the interaction between excimer laser beams and polymer surfaces[2,3]. Use of the XeCl* laser emitting at 308 nm is particularly attractive in view of high available pulse energies, reliability and ease of operation, and low operating costs[4]. In order to overcome the fact that many polymers, such as poly(methyl methacrylate) (PMMA), do not absorb in the region around 300 nm, several attempts have been reported to sensitize

[a] Present address: Bayer AG, D-47812 Krefeld-Uerdingen, Germany.
[b] Present address: National Institute of Materials and Chemical Research, Tsukuba, Ibaraki 305, Japan.

© 1995, Hüthig & Wepf Verlag, Zug CCC 1022-1352/95/$10.00

these polymers for 308 nm ablation, by adding a small amount of a chromophore like acridine[5], benzophenone[6] or 1,3-diphenyltriazenes[7,8]. Recently the ablation behaviour of PMMA doped with 1-aryl-3,3-diethyltriazene was characterized[9].

Results obtained with the latter approach have prompted us to study the ablation of polymers which contain photo-degradable functionalities in the polymer main chain itself[10]. In a preliminary report, the synthesis of a novel triazeno-group containing photopolymer was presented[11]. The favorable ablation characteristics of this material are discussed elsewhere[10,12]. Here we report on the synthesis and characterization of a series of triazene polymers, in which structural parameters are varied with the objective of optimizing material properties for photoreproduction techniques; eleven polymers were synthesized varying both aromatic substituents and alkyl substituents. Critical points for possible applications in photoresist techniques are the photolability and the thermostability of the triazene polymers (in prebaking and postbaking processes, temperatures up to 160 °C are used). In order to assess adequate stability of the developed materials, differential scanning calorimetry (DSC) and thermogravimetric analysis (TGA) measurements have been performed.

Results and discussion

The triazene polymers were synthesized by an interfacial polycondensation procedure in which a bis-diazonium salt reacts with a bifunctional aliphatic secondary amine. For a systematic study of the influence of structural parameters on the mentioned properties of the photopolymers, two series of polymers were synthesized. On the one hand the bifunctional amine was varied; on the other hand the bridging substituent between the two phenyl rings was changed, as shown in *Scheme 1*.

Scheme 1:

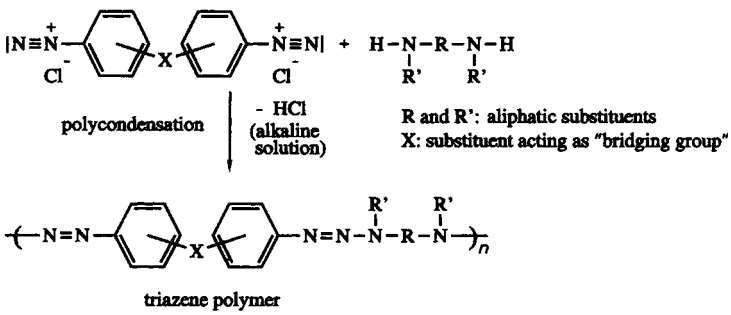

An overview of the synthesized triazene polymers is presented in Tab. 1. The polymers TP1–TP6 differ in the aliphatic part of the repeating unit; TP6–TP11 feature different bridging substituents between the aromatic rings.

Tab. 1. Structure of the synthesized triazene polymers

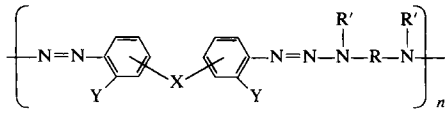

X	Y	R	R′	Polymer
p-O	H	$(CH_2)_2$	CH_3	TP1
p-O	H	$(CH_2)_2$	C_2H_5	TP2
p-O	H	$(CH_2)_3$	CH_3	TP3
p-O	H	$(CH_2)_3$	C_2H_5	TP4
p-O	H	$(CH_2)_4$	C_3H_7	TP5
p-O	H	$(CH_2)_6$	CH_3	TP6
p-CO	H	$(CH_2)_6$	CH_3	TP7
p-SO_2	H	$(CH_2)_6$	CH_3	TP8
m-SO_2	H	$(CH_2)_6$	CH_3	TP9
p-HC=CH	H	$(CH_2)_6$	CH_3	TP10
p-—	OMe	$(CH_2)_6$	CH_3	TP11

Measured molar masses of the triazene polymers determined by gel-permeation chromatography (GPC) in THF solution are presented in Tab. 2. The GPC curves were calibrated with PMMA standards. Although this calibration may give rise to systematic deviation from the correct molar masses, the results clearly indicate that high molar masses up to the range of number-average molar mass $\overline{M}_n = 15000\ g \cdot mol^{-1}$ can be reached in the synthesis. The high mass-average molar mass $\overline{M}_w$ values found for the

Tab. 2. Molar masses of the triazene polymers determined by gel-permeation chromatography (GPC) measurements

Polymer	$\overline{M}_n$ [a]	$\overline{M}_w$ [a]	$\overline{M}_{max}$ [a]
	g/mol	g/mol	g/mol
TP1	6 800	46 000	30 000
TP2	4 800	19 000	12 000
TP3	3 700	19 000	15 000
TP4	4 000	17 000	9 000
TP5	3 300	22 000	16 000
TP6	15 000	71 000	30 000
TP7	11 400	65 000	35 000
TP8	4 700	107 000 [b]	10 000
TP9	4 200	207 000 [b]	10 000
TP10	2 400	13 000	15 000
TP11	9 800	53 000	35 000

[a] $\overline{M}_n$, $\overline{M}_w$: number- and mass-average molar masses, resp., molar mass at the maximum of the GPC curve.

[b] The high molar mass of the polymers with SO_2 bridging groups may be due to partial association of polymer chains due to polar interactions.

Tab. 3. UV spectral characteristics of the triazene polymers

Polymer	λ_{max}/nm [a]	ε_{max}/(L · mol^{-1} · cm^{-1})
TP1	334	28 000
TP2	340	29 400
TP3	332	28 900
TP4	335	26 900
TP5	334	29 700
TP6	332	30 600
TP7	352	39 000
TP8	338	29 400
TP9	293	25 700
TP10	381	38 300
TP11	367	30 800

[a] Wavelength of the absorption maximum.

—SO_2— bridged polymers indicate the existence of high molar-mass fractions. The origin of this behaviour, which deviates from the one of the other investigated polymers, is awaiting further clarification. At present, the value of the molar mass determined at the maximum of the GPC curve (M_{max}) is considered as the best basis for a comparison of the triazene polymers.

The central point of interest is the photolytic decomposition of the triazene polymers. Spectral parameters of the triazene polymers measured in THF solution are summarized in Tab. 3. All polymers show a strong UV absorption maximum in the region between 293 nm (TP9) and 381 nm (TP10). This band is assigned to a π,π^*-transition, in agreement with the results of semiempirical AM1- and PM3-calculations on 1-aryl-3,3-diethyltriazenes[13].

For a quantification of the photolability of the synthesized triazene polymers, solutions in tetrahydrofuran were exposed to the polychromatic light of a high pressure xenon lamp. Typical concentrations were $\approx 10^{-6}$ M of polymer or $< 10^{-4}$ M of chromophore, depending on the sample; the decomposition was followed by UV spectroscopy. Representative results for the decomposition of polymer TP2 are shown in Fig. 1. UV spectra were recorded after the polymer solution had been exposed to the light of the UV lamp for subsequent intervals of 10 s each.

Owing to the high absorption, the decomposition proceeds according to zero-order kinetics during the initial stages of the photolysis, and according to first-order kinetics after absorbance has fallen below $\approx 0{,}5$. From the latter part of the experiments, reaction rate constants were calculated by using the Guggenheim method[14]. As the rate is proportional to the intensity of the UV light source used in the given experiment, only relative values of the rate constants are of interest for comparing the photochemical reactivity of the various materials. A comparison of the triazene polymers TP6–TP11, which differ in the substituent X bridging the aromatic rings, is presented in Fig. 2. For a substitution pattern where X is in *para*-position with respect to the triazeno group, electron-withdrawing groups such as CO or SO_2 are seen to give rise

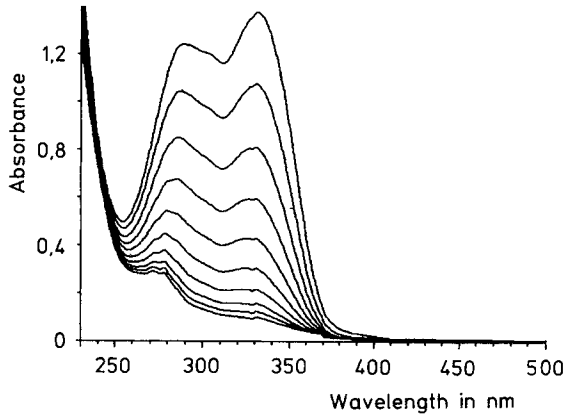

Fig. 1. Photolysis of TP2 in THF solution. UV spectra were recorded after successive exposures, of 10 s each, to the light of a xenon lamp, as described in the text

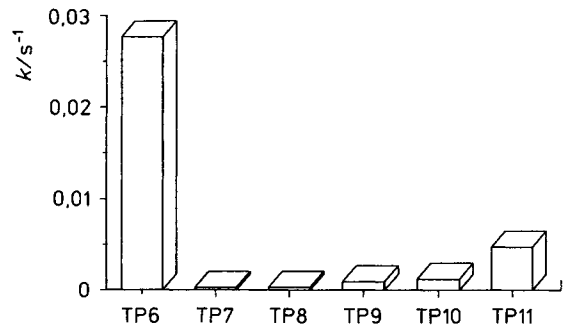

Fig. 2. Reaction rate constants for the photolysis of the triazene polymers with different aromatic substituents (TP6–TP11), as calculated using the Guggenheim approximation

to lower photolysis reaction rates, as compared to the electron-donating oxygen bridge in polymer TP6. In the polymer TP11 in which the phenyl rings are directly connected, an electron-donating OCH_3 substituent in *ortho*-position again gives rise to a comparatively high photolysis rate. This effect is analogous to trends that were earlier observed in the photolysis of 1-aryl-3,3-diethyltriazene[15].

Effect of a variation in the alkyl part of the polymer on the photolysis reaction rate constant were studied for the case of the most photosensitive triazene polymer mentioned so far, i. e. TP6. To this aim, the polymers TP1–TP5 were synthesized using various bifunctional secondary amines. Again, the photolysis of these triazene polymers was monitored by UV spectroscopy, and photolysis reaction rate constants were calculated using the Guggenheim approximation. As seen in Fig. 3, the photolysis reaction rate constants vary signficantly within the series of triazene polymers TP1–TP6; from the results, two trends may be identified.

First, introduction of alkyl substituents R′ with increasing steric demand (replacement of a methyl- by an ethyl- or propyl group) results in an increasing efficiency of the photolytic decomposition, by decreasing the ability of recombination of the formed

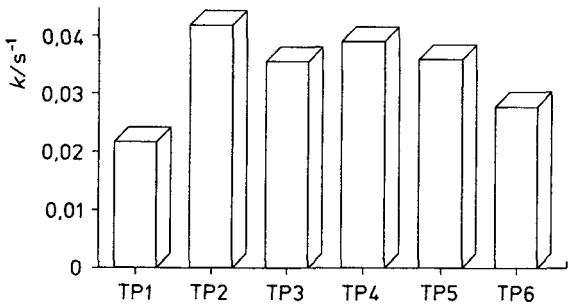

Fig. 3. Reaction rate constants for the photolysis of the triazene polymers differing in the alkyl substituents (TP1–TP6), as calculated by using the Guggenheim approximation

radicals. This effect has been investigated intensively in case of thermolabile azo-compounds used as source of radicals in polymerization reactions.

Second, the differences in the photolysis reaction rate constants may be related to inductive effects increasing from methyl to propyl groups, and from ethylene to tetramethylene chains bound to the N^3 atom of the triazene functionality. This increasing inductive effect leads to a stabilization of the radicals formed during photolysis. Apparently the β-carbon atom has a pronounced effect, which levels off on introduction of a γ-carbon atom (TP5, TP6).

For the envisaged use of the triazene polymers in microlithography and, in particular, as photoresists in microchip technology, it is of upmost importance that the materials are stable at temperatures used in prebaking and postbaking processes. Therefore, the thermostability of the triazene polymers was investigated using DSC and TGA methods. All polymers show a surprisingly high thermostability, up to temperatures as high as 230 °C.

The thermolysis of the triazene polymers measured by TGA proceeds along two alternative pathways, as exemplified by the typical TGA traces shown in Fig. 4. The polymer TP6 (Fig. 4a) decomposes in a one-step reaction, in which both nitrogen and the bifunctional secondary amine are released. Provided that these are the only volatile species, the weight loss of the polymer at the decomposition temperature should not exceed the stoichiometric fractions of the amine and nitrogen. The observed weight loss of 62% is very close to the value calculated on the basis of these assumptions (54%). In contrast to this behaviour, TP11 exhibits a two-step decomposition (Fig. 4b). First two nitrogen molecules per repeating unit are released at a lower temperature, with an observed weight loss of 17%; subsequently, the aliphatic amine is liberated at a higher temperature with a weight loss of 39%.

Depending on the chemical structure, the glass transition temperatures of the triazene polymers vary from values close to room temperature to values well above 100 °C (Tab. 4). Both variation of the bridging substituent X (*Scheme 1*) and of the aliphatic amine have a strong effect on the glass temperature. Substituents like —HC=CH— (TP9), or the introduction of a direct chemical bonding betweeen the two phenyl groups (which increases the stiffness of the aromatic unit) are seen to raise the glass temperature. Even higher temperatures are observed for the polymers with electron-withdrawing —CO— or —SO_2— substituents, which lead to charge shifts

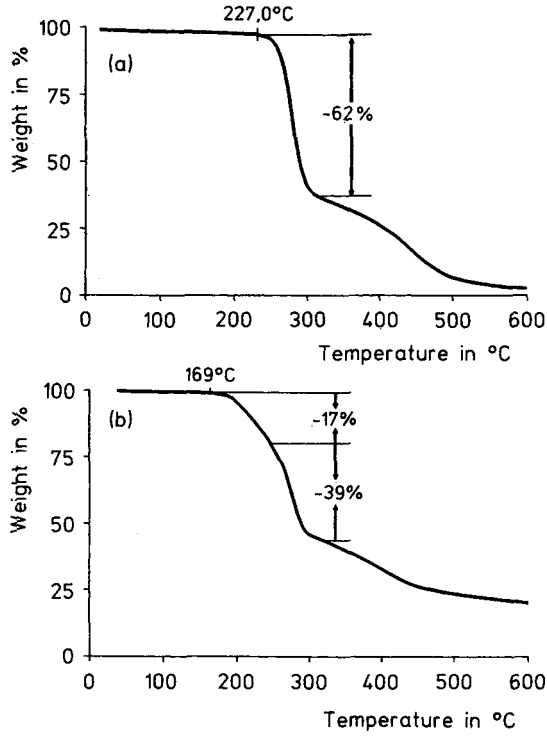

Fig. 4. Characterization of triazene polymers by thermogravimetric analysis (TGA): (a) TGA of TP6, showing a single decomposition step; (b) TGA of TP11, showing loss of nitrogen and aliphatic amine in two successive steps

Tab. 4. Thermochemical properties of the synthesized triazene polymers derived from differential scanning calorimetry (DSC) and thermogravimetric analysis (TGA) measurements

Polymer	T_{dec}/°C[a] (DSC)	ΔH_{dec}/ (kJ · mol^{-1})	T_{dec}/°C[b] (TGA)	T_g/°C[c]
TP1	274	−292,2	227	84
TP2	273	−206,2	205	60
TP3	275	−254,5	209	68
TP4	270	−205,9	188	45
TP5	224	−221,5	142	33
TP6	282	−255,1	227	63
TP7	300	−254,8	203	88
TP8	294	−257,2	213	110
TP9	300	−258,0	217	85
TP10	230	−225,5	195	76
TP11	221	−258,0	169	80

[a] Temperature at the maximum of the exothermic peak in the DSC curve (heating rate: 10 K/min).
[b] Beginning of weight loss (heating rate: 10 K/min).
[c] Glass transition temperature measured at a heating rate of 30 K/min.

within the triazeno group and an associated increase in the 1,3-dipolar character of this functionality. (The latter effect was extensively characterized for low-molar-mass triazene compounds[13]).

The glass transition temperature is decreased by increasing the steric demand of the alkyl substituent R at the nitrogen atom N^3 (cf. *Scheme 1*), i.e. by changing from a methyl to propyl substituent. This effect is of higher significance than the addition of methylene spacer groups between the triazeno groups.

Further thermochemical characterization data from DSC and TGA measurements are summarized in Tab. 4. As opposed to the high sensitivity to UV light, the triazene polymers show a remarkably high thermostability. Decomposition temperatures (defined as the maximum of the DSC curve) range up to 300 °C, and exhibit only a slight dependence on the type of the aliphatic amine. (Polymers TP5 and TP11, with decomposition temperatures around 220 °C, represent exceptions). Evidently, a change of the substituent between the two benzene rings from oxygen to more electrophilic groups, like carbonyl or sulfonyl, leads to an increase of the thermostability of the triazene polymer. This fact can be explained with the increasing dipolar character of the triazene group.

Conclusions

The syntheses, photolytic and thermal properties of eleven triazeno-group containing photopolymers were reported in the present paper. These polymers were prepared by an interfacial polycondensation reaction of a bis-diazonium salt and a bifunctional secondary amine. The resulting relatively high-molar-mass polymers are soluble in common organic solvents.

In the photolytic decomposition studies, a strong influence of the aromatic substituents on the reaction rate was derived. Aromatic substituents with electron-donating groups lead to highly photosensitive triazene polymers. On the other hand, triazene polymers with electron-withdrawing aromatic substituents show a significant higher stability against photolytic decomposition. The influence of the alkyl parts of the triazene polymers on the photolability is of smaller signficance, and can be explained in terms of inductive and steric effects of bulky alkyl substituents bonded to the N^3-nitrogen of the triazene function.

All triazene polymers show a remarkably high thermostability; thermal decomposition takes place at temperatures up to 300 °C. Both aromatic and alkyl substituents have a signficant influence on the glass transition temperatures of the triazene polymers. Bulky alkyl groups and flexible aromatic parts lead to lower glass transition temperatures, whereas electron-withdrawing aromatic substituents give rise to higher glass transition temperatures. In summary, the triazene polymers represent thermally stable, highly photosensitive materials for the use in photoreproduction, laser surface structuring, and microlithography techniques.

Experimental part

Apparatus

IR spectroscopy: Digilab FTS-40 (FT-IR).
^1H *NMR:* Bruker AC 250 (250 MHz).
^{13}C *NMR:* Bruker AC 250 (62,5 MHz).
Gel-permeation chromatography (GPC): Waters, Mod. 590 (UV_{254}, RI detector); eluent tetrahydrofuran (THF); calibration with poly(methyl methacrylate) standards; columns: 500, 10^3, 10^4, 10^5 Å.
Differential scanning calorimetry (DSC): Perkin-Elmer DSC 7 (T_g measurements), Netzsch DSC 200 (thermolysis, thermolysis-kinetic).
UV/Vis spectroscopy: Hitachi U-3000 UV spectrometer.
UV lamp: LTI Mod. A 1020, 150 W Xenon high pressure lamp.
Thermogravimetric analysis (TGA) measurements: Netzsch Simultan-Thermoanalyse STA 409C.

Synthesis

The triazene polymers were synthesized according to the procedure described in detail elsewhere[11].

Characterization

a) TP1
Yield: 1,14 g (37% of theoretical yield, polymer not quantitatively soluble in THF).
IR (KBr): 1395 (N=N), 1234 (C—O), 1587 cm^{-1} (aromatic system).
UV/Vis (THF): λ_{max}/nm (ε/(L · mol^{-1} · cm^{-1})): 334 (28000).
^1H NMR ($CDCl_3$): δ = 6,85–7,4 (m; 8H, Ar); 4,0 (m; 4H, N—CH_2—); 3,25 (s; 6H, N—CH_3).
GPC (THF), MW in g/mol: 6800 ($\bar{M}_n$), 46000 ($\bar{M}_w$).
DSC: T_g: 84 °C, T_{dec}: 276 °C, ΔH_{dec}: 292,2 kJ/mol.
TGA: T_{start}: 227 °C, one step (weight loss 58%).

b) TP2
Yield: 1,47 g (43% of theoretical yield, polymer not quantitatively soluble in THF).
IR (KBr): 1402 (N=N), 1234 (C—O), 1587 cm^{-1} (aromatic system).
UV/Vis (THF): λ_{max}/nm (ε/(L · mol^{-1} · cm^{-1})): 340 (29400).
^1H NMR ($CDCl_3$): δ = 6,95–7,45 (m; 8H, Ar); 3,95 (m; 4H, N—$\underline{CH_2}$—$\underline{CH_2}$—N); 3,75 (q; 4H, N—$\underline{CH_2}$—CH_3); 12,5 (t; 6H, N—CH_2—$\underline{CH_3}$).
GPC: (THF), MW in g/mol: 4800 ($\bar{M}_n$), 19000 ($\bar{M}_w$).
DSC: T_g: 60 °C, T_{dec}: 273 °C, ΔH_{dec}: −206,2 kJ/mol.
TGA: T_{start}: 218 °C, one step (weight loss 48%).

c) TP3
Yield: 1,32 g (41% of theoretical yield).
IR (KBr): 1395 (N=N), 1233 (Ar—O), 1587 cm^{-1} (aromatic system).
UV/Vis (THF): λ_{max}/nm (ε/(L · mol^{-1} · cm^{-1})): 332 (28900).
^1H NMR ($CDCl_3$): δ = 6,9–7,45 (m; 8H, Ar); 3,75 (t; 4H, N—CH_2—); 3,2 (s; 6H, N—CH_3); 2,1 (m; 2H, N—CH_2—$\underline{CH_2}$—).
GPC (THF), MW in g/mol: 3700 ($\bar{M}_n$), 19000 ($\bar{M}_w$).
DSC: T_g: 68 °C, T_{dec}: 275 °C, ΔH_{dec}: −254,5 kJ/mol.
TGA: T_{start}: 220 °C, one step (weight loss 55%).

d) TP4

Yield: 1,50 g (43% of theoretical yield).
IR (KBr): 1402 (N=N), 1229 (Ar—O), 1587 cm^{-1} (aromatic system).
UV/Vis (THF): λ_{max}/nm (ε/(L · mol^{-1} · cm^{-1})): 335 (26900).
^{1}H NMR ($CDCl_3$): δ = 6,9–7,4 (m; 8H, Ar); 3,65–3,85 (m; 8H, N—$\underline{CH_2}$—); 2,1 (m; 2H, N—CH_2—$\underline{CH_2}$—); 1,25 (t; 6H, N—CH_2—$\underline{CH_3}$).
GPC (THF), MW in g/mol: 4000 ($\bar{M}_n$), 17000 ($\bar{M}_w$).
DSC: T_g: 45 °C, T_{dec}: 270 °C, ΔH_{dec}: −205,9 kJ/mol.
TGA: T_{start}: 175 °C, one steps (weight losses 13 and 35%).

e) TP5

Yield: 1,82 g (46% of theoretical yield).
IR (KBr): 1400 (N=N), 1236 (Ar—O), 1587 cm^{-1} (aromatic system).
UV/Vis (THF): λ_{max}/nm (ε/(L · mol^{-1} · cm^{-1})): 334 (29700).
^{1}H NMR ($CDCl_3$): δ = 6,9–7,45 (m; 8H, Ar); 3,7 (m; 4H, N—$\underline{CH_2}$—); 3,6 (t; 4H, N—$\underline{CH_2}$—CH_2—CH_3); 1,6–1,8 (m; 8H, N—CH_2—$\underline{CH_2}$—); 0,9 (t; 6H, —CH_3).
GPC (THF), MW in g/mol: 3300 ($\bar{M}_n$), 22000 ($\bar{M}_w$).
DSC: T_g: 33 °C, T_{dec}: 233 °C, ΔH_{dec}: −221,5 kJ/mol.
TGA: T_{start}: 195 °C, one step (weight loss 47%).

f) TP6

Yield: 2,32 g (63% of theoretical yield).
IR (KBr): 1401 (N=N), 1234 (Ar—O), 1587 cm^{-1} (aromatic system).
UV/Vis (THF): λ_{max}/nm (ε/(L · mol^{-1} · cm^{-1})): 332 (30600).
^{1}H NMR ($CDCl_3$): δ = 6,85–7,4 (m; 8H, Ar); 3,7 (t; 4H, N—CH_2—); 3,1 (s; 6H, N—CH_3—); 1,65 (m; 4H, N—CH_2—$\underline{CH_2}$—); 1,35 (m; 4H, N—CH_2—CH_2—$\underline{CH_2}$—).
GPC: (THF), MW in g/mol: 15000 ($\bar{M}_n$), 71000 ($\bar{M}_w$).
DSC: T_g: 63 °C, T_{dec}: 282 °C, ΔH_{dec}: −255,1 kJ/mol.
TGA: T_{start}: 227 °C, one step (weight loss 62%).

g) TP7

Yield: 3,08 g (81% of theoretical yield).
IR (KBr): 1389 (N=N), 1645 (C=O), 1595 (aromatic system).
UV/Vis (THF): λ_{max}/nm (ε/(L · mol^{-1} · cm^{-1})): 352 (39000).
^{1}H NMR ($CDCl_3$): δ = 7,3–7,8 (m; 8H, Ar); 3,75 (m; 4H, N—CH_2—); 3,2 (s; 6H, N—CH_3); 1,65 (m; 4H, N—CH_2—$\underline{CH_2}$—); 1,35 (m; 4H, N—CH_2—CH_2—$\underline{CH_2}$—).
GPC (THF), MW in g/mol: 11400 ($\bar{M}_n$), 65000 ($\bar{M}_w$).
DSC: T_g: 88 °C, T_{dec}: 300 °C, ΔH_{dec}: −254,8 kJ/mol.
TGA: T_{start}: 203 °C, one step (weight loss 45%).

h) TP8

Yield: 2,07 g (50% of theoretical yield, polymer not quantitatively soluble in THF).
IR(KBr): 1385 (N=N), 1148 (SO_2), 1587 cm^{-1} (aromatic system).
UV/Vis (THF): λ_{max}/nm (ε/(L · mol^{-1} · cm^{-1})): 338 (29400).
^{1}H NMR ($CDCl_3$)): δ = 7,35–7,85 (m; 8H, Ar); 3,7 (m; 4H, N—CH_2—); 3,1 (s; 6H, N—CH_3); 1,6 (m; 4H, N—CH_2—$\underline{CH_2}$—); 1,3 (m; 4H, N—CH_2—Ch_2—$\underline{CH_2}$—).
GPC (THF), MW in g/mol: 4700 ($\bar{M}_n$), 107000 ($\bar{M}_w$).
DSC: T_g: 110 °C, T_{dec}: 294 °C, ΔH_{dec}: −257,2 kJ/mol.
TGA: T_{start}: 213 °C, one step (weight loss 35%).

i) TP9

Yield: 2,47 g (60% of theoretical yield).
IR (KBr): 1391 (N=N), 1142 (SO_2), 1589 cm^{-1} (aromatic system).
UV/Vis (THF): λ_{max}/nm (ε/(L · mol^{-1} · cm^{-1})): 293 (25700).

^{1}H NMR ($CDCl_3$): δ = 7,2–8,0 (m; 8H, Ar); 3,7 (t; 4H, N—CH_2—); 3,1 (s; 6H, N—CH_3); 1,65 (m; 4H, N—CH_2—$\underline{CH_2}$—); 1,35 (m; 4H, N—CH_2—CH_2—$\underline{CH_2}$—).
GPC (THF), MW in g/mol: 4200 ($\bar{M}_n$), 207000 ($\bar{M}_w$).
DSC: T_g: 85 °C, T_{dec}: 300 °C, ΔH_{dec}: −258,0 kJ/mol.
TGA: T_{start}: 217 °C, one step (weight loss 38%).

j) TPI0

Yield: 1,29 g (34% of theoretical yield, polymer not quantitatively soluble in THF).
IR (KBr): 1391 (N=N), 1597 cm^{-1} (aromatic system).
UV/Vis (THF): λ_{max}/nm (ε/(L · mol^{-1} · cm^{-1})): 381 (38300).
^{1}H NMR ($CDCl_3$): δ = 7,25–7,5 (m; 8H, Ar); 7,0 (s; 2H, —HC=CH—); 3,7 (m; 4H, N—CH_2—); 3,2 (s; 6H, N—CH_3); 1,65 (m; 4H, N—CH_2—$\underline{CH_2}$—); 1,35 (m; 4H, N—CH_2—CH_2—$\underline{CH_2}$—).
GPC (THF), MW in g/mol: 22400 ($\bar{M}_n$), 13000 ($\bar{M}_w$).
DSC: T_g: 76 °C, T_{dec}: 230 °C, ΔH_{dec}: −225,2 kJ/mol.
TGA: T_{start}: 195 °C, one step (weight loss 36%).

k) TPI1

Yield: 2,48 g (60% of theoretical yield).
IR (KBr): 1387 (N=N), 1240 (N—N), 1562 cm^{-1} (aromatic system).
UV/Vis (THF): λ_{max}/nm (ε/(L · mol^{-1} · cm^{-1})): 367 (30800).
^{1}H NMR ($CDCl_3$): δ = 7,1–7,4 (m; 6H, Ar); 3,95 (s; 6H, OCH_3); 3,75 (t; 4H, N—CH_2 —); 3,25 (s; 6H, N—CH_3); 1,7 (m; 4H, N—CH_2—$\underline{CH_2}$—); 1,4 (m; 4H, N—CH_2—CH_2—$\underline{CH_2}$—).
GPC (THF), MW in g/mol: 9800 ($\bar{M}_n$), 53000 ($\bar{M}_w$).
DSC: T_g: 80 °C, T_{dec}: 212/272 °C, ΔH_{dec}: −258,1 kJ/mol.
TGA: T_{start}: 169 °C, two steps (weight losses 17 and 39%).

[1] J. F. Rabek, *Mechanisms of Photophysical Processes and Photochemical Reactions in Polymers,* John Wiley & Sons, Chichester 1987
[2] R. Srinivasan, B. Braren, *Chem. Rev.* **89**, 1303 (1989)
[3] S. Lazare, V. Granier, *Laser Chem.* **10**, 25 (1989)
[4] K. Jain, *Excimer Laser Lithography,* SPIE, Bellingham 1990
[5] R. Srinivasan, B. Braren, R. W. Dreyfus, L. Hadel, D. E. Seeger, *J. Opt. Soc. Am.: Opt. Phys.* **B3**, 785 (1986)
[6] H. Masuhara, H. Hiraoka, K. Domen, *Macromolecules* **20**, 452 (1987)
[7] M. Bolle, K. Luther, J. Troe, J. Ihlemann, H. Gerhardt, *Appl. Surf. Sci.* **46**, 279 (1990)
[8] J. Ihlemann, M. Bolle, K. Luther, J. Troe, in: *Physical Concepts of Materials for Novel Optoelectronic Device Applications I,* SPIE-Proc. vol. 1361, Bellingham 1990
[9] T. Lippert, A. Wokaun, J. Stebani, O. Nuyken, J. Ihlemann, *Angew. Makromol. Chem.* **213**, 127 (1993)
[10] T. Lippert, A. Wokaun, J. Stebani, O. Nuyken, J. Ihlemann, *Angew. Makromol. Chem.* **206**, 97 (1993)
[11] J. Stebani, O. Nuyken, T. Lippert, A. Wokaun, *Makromol. Chem., Rapid Commun.* **14**, 365 (1993)
[12] T. Lippert, J. Stebani, J. Ihlemann, O. Nuyken, A. Wokaun, *J. Phys. Chem.* **97**, 12296 (1993)
[13] J.-C. Panitz, T. Lippert, J. Stebani, J. Ihlemann, O. Nuyken, A. Wokaun, *J. Phys. Chem.* **97**, 5246 (1993)
[14] E. A. Guggenheim, *Philos. Mag.* **2**, 538 (1926)
[15] T. Lippert, J. Stebani, A. Stasko, O. Nuyken, A. Wokaun, *J. Photochem. Photobiol.* **78**, 139 (1994)